# Università degli Studi di Napoli "Federico II"



# SCUOLA POLITECNICA E DELLE SCIENZE DI BASE DIPARTIMENTO DI INGEGNERIA INDUSTRIALE

# CORSO DI LAUREA IN INGEGNERIA AEROSPAZIALE CLASSE DELLE LAUREE IN INGEGNERIA INDUSTRIALE (L-9)

# Elaborato di laurea in Meccanica del Volo Performance evaluation of a UAM aircraft in fixedwing configuration with MATLAB live script

Relatore: Prof. Danilo Ciliberti Candidato: Camilla Pullano Matr. N35004354

A chi ogni giorno si perde nei propri pensieri e nelle domande senza risposte, eppur non smette di sognare.

# Abstract

The objective of this paper is to determine and subsequently analyze the performance of a fixed-wing UAM aircraft, therefore not with vertical take-off and landing, but rather horizontal. In the first part, the concept of UAM is introduced, with eVTOLs being the absolute protagonists. The applications, challenges, and risks characterizing the complexity of these aircraft are then analyzed, while also highlighting their innovation and sustainability. The different types of aircraft designed to be as functional as possible for the intended use are examined in depth, along with the concept of electric propulsion. Finally, the infrastructures that will host these vehicles and the management of airspace are mentioned, as these aspects are necessary to ensure safe and reliable operation. In the following chapters, the Matlab Live Script code is presented, through which the performance analysis of the aircraft was carried out. The input data of the selected aircraft, equipped with a Rotax 916 iS engine (160 hp), are then reported, followed by the results obtained, with a brief consistency and reliability check. To conclude, a brief parametric study of the performance was conducted by varying the zero-lift drag coefficient, also referred to as parasite drag.

# **Sommario**

L'obiettivo di questo elaborato è quello di determinare e in seguito analizzare le prestazioni di un velivolo UAM ad ala fissa, dunque non con decollo e atterraggio verticale, bensì orizzontale. Nella prima parte viene introdotto il concetto di UAM, che vede come protagonisti assoluti gli eVTOL. Sono di seguito analizzati gli impieghi, le sfide e i rischi che caratterizzano la complessità di questi aeromobili, evidenziandone al contempo l'innovazione e la sostenibilità. Sono approfondite le differenti tipologie di velivoli progettati per essere il più possibile funzionali al tipo di utilizzo previsto, e il concetto di propulsione elettrica. Infine, sono citate le infrastrutture che ospiteranno tali mezzi e la gestione degli spazi, aspetti necessari a garantire un funzionamento in totale sicurezza e affidabilità. Nei successivi capitoli viene presentato il codice Matlab Live Script con cui è stato possibile effettuare l'analisi delle prestazioni del velivolo. Sono riportati, dunque, i dati in input del velivolo scelto, con motore Rotax 916 iS (160 hp), e successivamente i risultati ottenuti, seguiti da una breve verifica di coerenza e attendibilità. Per concludere è stato condotto un piccolo studio parametrico delle performance al variare del coefficiente di resistenza aerodinamica a portanza nulla, ovvero della resistenza parassita.

# **Table of contents**

1.	UR	BAN AIR MOBILITY	6
	1.1	The UAM Concept	6
	1.2	Typical Missions	7
	1.2.	.1 Passenger transport	7
	1.2.	.2 Cargo transport / goods delivery	8
	1.2.	.3 Emergency / medical flights	8
	1.3	Typical Configurations	9
	1.3.	.1 Vectored Thrust	9
	1.3.	.2 Lift + cruise	10
	1.3.	.3 Wingless / Multicopter	10
	1.4	UAM Challenges	10
	1.4.	.1 Infrastructure	11
	1.4.	.2 Social acceptance	12
	1.4.	.3 Safety	13
	1.4.	.4 Technology and Electric Propulsion	14
	1.5	UAM Risks	15
	1.6	The concept of airspace "ownership"	16
2.	MA	ATLAB LIVE SCRIPT	17
	2.1	The updated script	17
	2.2	"AllData" Struct	18
	2.2.	.1 Aircraft and Atmosphere Input Data	19
3.	AIF	RCRAFT PERFORMANCE EVALUATION	23
	3.1	Technical polar	23
	3.2	Propulsive characteristics	24
	3.3	Climb, Descent and Glide	25

	3.3	.1	Best CLIMB	25
	3.3	.2	Actual Climb	25
	3.3.3		Controlled Climb	25
	3.3.4		Controlled Descent	25
	3.3	.5	Ceiling AEO	26
	3.3	.6	Climb flight time	26
	3.4	Lev	el Flight	26
	3.5	Aut	tonomies	27
	3.6	Tak	ke-off	28
	3.7	Lan	nding	28
	3.8	Tur	n	28
	3.8	.1	Best Turn	29
	3.8	.2	Actual Turn	29
	3.9	Infl	luence of Parasite Drag on Performance	29
	3.9	.1	Influence on Maximum Efficiency	30
	3.9	.2	Influence on Maximum Speed	30
	3.9	.3	Influence on Maximum Rate of Climb	31
	3.9	.4	Influence on Maximum Endurance	32
	3.9	.5	Influence on Maximum Range	33
	3.9	.6	Influence on Maximum Range in Glide	33
4.	Cor	nclus	sion	34

# **List of figures**

Figure 1.1 – Number of passenger drones in UAM operation worldwide [9]	8
Figure 1.2 – UAM vehicle types [4]	9
Figure 1.3 – Challenges for UAM, in percentage [4]	11
Figure 1.4 – UAM infrastructure: scalable vertiport types [4]	12
Figure 1.5 – Societal acceptance factors, in percentage [4]	13
Figure 1.6 – Technology scenarios [5]	15
Figure 2.1 – AllData's first level [6]	18
Figure 2.2 – Plot of <i>CD</i> VS <i>CL2</i> for the calculation of the Oswald efficiency factor	21
Figure 2.3 – Complete aircraft with propellers	22
Figure 3.1– Maximum performance values as a function of <i>CD</i> 0	30
Figure 3.2 – Maximum Efficiency vs. <i>CD</i> 0	30
Figure 3.3 – Maximum Speed vs. <i>CD</i> 0	31
Figure 3.4 – Rate of climb max vs. <i>CD</i> 0	31
Figure 3.5 – Endurance max vs. <i>CD0</i>	32
Figure 3.6 – Maximum Range vs. <b>CD0</b>	33
Figure 3.7 – Maximum Range in Glide vs. CD0	33

# 1. URBAN AIR MOBILITY

# 1.1 The UAM Concept

Urban Air Mobility (UAM) was born in a historical period in which the growth of populations in megacities, the resulting constant increase in pollution, traffic, and discomfort, are pushing to the limit and endangering the quality of life of humans. By 2030, it is predicted that 60% of the global population will live in urban agglomerations, a percentage that is destined to increase, reaching as much as three-quarters of the world's population by 2050. Cities will be responsible for 70% of greenhouse gas emissions and will consume two-thirds of global energy resources [2].

The third dimension, that is, the air, is undoubtedly the solution to be pursued in the not-sodistant future.

UAM is part of a broader initiative, promoted by NASA, FAA (Federal Aviation Administration), and the companies in the sector, called Advance Air Mobility (AAM). This system involves the transportation of people and goods, both within cities (intra-urban mobility) and between different cities (inter-urban mobility).

Thus, UAM aims to promise a faster, more ecological, and safer transportation system. Although it may seem like a concept still far from our daily lives, projects and trials are already taking place worldwide. A concrete example of UAM is the passenger service launched in May 2019 in China by the company EHang. This connected a port to a hotel on an island, reducing the travel time from 40 minutes by road to just 5 minutes by air, marking a milestone in the development of this sector [7].

UAM aims to create compact, agile, and autonomous aircraft, with a particular focus on those with vertical takeoff and landing capabilities, eVTOLs (Electric Vertical Take-Off and Landing). Not by chance, as a concept, UAM has been defined by NASA as "safe and efficient air traffic operations in a metropolitan area for manned aircraft and unmanned aircraft systems" [7].

Although unmanned aerial systems (UAS) already exist today, unmanned air vehicles (UAVs), or commonly drones, are designed for different purposes, such as fire detection, traffic monitoring, and more.

# 1.2 Typical Missions

In the context of UAM (Urban Air Mobility), as we have already seen, we are referring to the implementation of innovative solutions for smart mobility, which involves the use and optimization of technologies that are eco-friendly, quiet, and, above all, safe.

The sector is also evolving on multiple fronts, with the development of approaches that include both direct control by a pilot and remote piloting technologies, which can operate either within visual line of sight (VLoS) or beyond the line of sight (BLoS) [2].

However, although UAM refers to all transport vehicles designed for very short-range aerial travel and at low altitude (below 5,000 feet / 1,500 meters above ground level), autonomous flight still appears to be a particularly challenging issue when it comes to passenger transport [2].

# 1.2.1 Passenger transport

Commercial passenger transport involves a number of passengers ranging from one to six and may include [11]:

- flights between the city center and an airport;
- sightseeing flights within the city;
- flights within a metropolitan area.

As already mentioned, most manufacturers aim to begin this type of operation with pilots on board.

Figure 1.1 shows the projected evolution of the number of passenger drones used in UAM operations from 2020 to 2050, with air taxis representing the segment expected to grow the most each year [9].

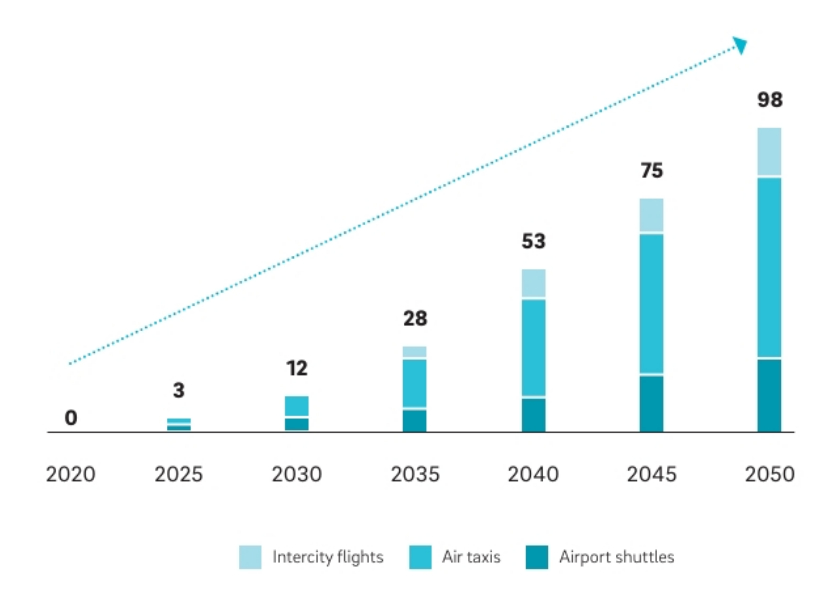


Figure 1.1 – Number of passenger drones in UAM operation worldwide [9]

# 1.2.2 Cargo transport / goods delivery

Cargo transport using UAM aircraft can be intended for commercial or industrial purposes, with payloads ranging from 0.7 to 200 kg. Some vehicles will be remotely controlled, while others are being developed to operate autonomously from the beginning [11].

Key examples in this sector include [11]:

- last mile delivery;
- delivery to a hub;
- rural delivery of supplies.

Moreover, efforts are being made to identify locations where such deliveries can be safely ensured, such as near a station, on a rooftop, or in a garden, where available.

# 1.2.3 Emergency / medical flights

This field can include applications such as [11]:

- transport of emergency medical personnel to the accident site;
- transport of patients to the hospital;
- transport of emergency goods and medical supplies;

- assessment of emergency areas;
- direct assistance during fire incidents.

The last three use cases mentioned above can be handled by unmanned drones; moreover, both passenger transport and cargo delivery aircraft can, if necessary, be used for emergency missions.

# 1.3 Typical Configurations

As previously mentioned, the central elements of UAM are the so-called eVTOLs, aircraft capable of hovering, taking off, and landing vertically. They differ from traditional helicopters in that the engine and rotors are replaced by a distributed electric propulsion (DEP) system, which powers smaller rotors. Currently, there are three main types of eVTOLs, each with specific features and advantages depending on the mission for which they are designed, such as travel within cities or between different urban areas [13].

These three models are based on similar design solutions, although they differ in terms of technical configuration, operating costs, and range, as we can see in Figure 1.2 [4].



Figure 1.2 – UAM vehicle types [4]

#### 1.3.1 Vectored Thrust

In this type of aircraft, the thrust required for lift during the hover phase and thrust during the cruise phase is generated by the same propulsion units, as the rotating elements can change orientation, shifting from vertical to horizontal [4][2].

During the cruise phase, lift is in fact provided by the wings with which the aircraft is equipped, and it can reach speeds of up to 300 km/h with a range of 300 km [2].

This configuration is considered the most suitable for long-distance flights; in particular, vectored thrust appears to be the best choice for passenger transport. However, its main limitation stems from the engine redundancy required to ensure an adequate level of safety; this, in turn, increases weight, cost, and certification complexity [4].

$$1.3.2$$
 Lift + cruise

This configuration, on the other hand, features separate propulsion units for the hover and cruise phases, and during the latter, lift is generated by the wings [4].

It is better suited for short-distance operations and cargo transport, with a payload capacity ranging from 0.7 to 200 kg [4][2].

It is also easier to certify, due to the separation of the propulsion systems [4].

# 1.3.3 Wingless / Multicopter

The propulsion units are fixed and generate continuous lift. This system is suited to even shorter distances than lift + cruise configurations, and from an engineering perspective, it represents the simplest concept, as it avoids any unnecessary moving components [4].

The speed is low, around 90 km/h, but these vehicles are highly efficient and quiet, with an operational range of 40–50 km [2].

They are well suited for emergency scenarios, such as the transport of medical personnel or patients to hospitals, or, as previously mentioned, for direct intervention in firefighting operations [4].

# 1.4 UAM Challenges

Figure 1.3 shows the main challenges expected for Urban Air Mobility. At the top of the list are infrastructure, safety, noise and environmental impact, and the technologies employed. The latter mainly refer to the innovative use of electric propulsion systems, whose main challenge is the so-called "SWaP riddle" [2], an acronym for Size, Weight, and Power, thus referring to the balance between power, lightness, and dimensions. Moreover, the term "environmental"

impact" encompasses a broader range of aspects, including air, visual, and noise pollution, land use, species protection, climate, and natural resources [4].

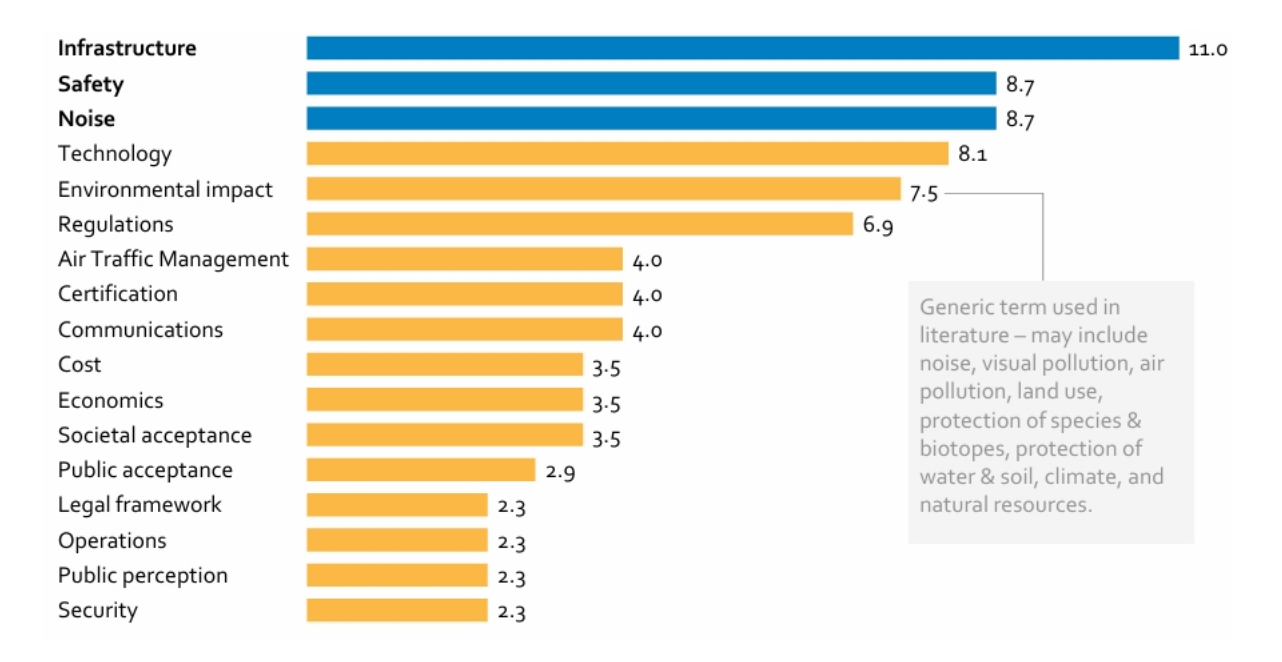


Figure 1.3 – Challenges for UAM, in percentage [4]

These are factors previously mentioned, confirming their relevance within the context of Urban Air Mobility, which is emerging as the next generational leap in urban transportation. The goal is not only to improve the environmental quality of urban spaces, but also to expand the range of mobility, enabling significantly greater distances to be covered in the same amount of time (for instance, compared to a car).

## 1.4.1 Infrastructure

Infrastructure is a fundamental component for enabling the operation of air mobility. Among these, vertiports stand out, facilities specifically designed to support the take-off and landing of UAM vehicles. Two critical factors in their design and location are user accessibility and the availability of reliable connections to the electrical grid. Indeed, efficient integration with the urban energy infrastructure is essential, as air taxi recharging is expected to take place at these sites. Furthermore, the size and number of vertiports may vary from city to city, depending on projected traffic volumes. Each urban area will host a different combination of vertiports, each equipped with a variable number of landing pads: from vertipads, with one or two pads, to vertihubs, which may accommodate up to ten [4].

Figure 1.4 presents potential configurations of UAM networks in various types of cities, indicating for each the estimated number of vertiports and their respective landing capacities. The anticipated distribution suggests that larger facilities will be fewer in number, while smaller ones will be more widely dispersed across the territory.

Large cities			Medium cities			
Large, dense, high-income urbai Paris, Berlin, Madrid, Hamburg, Barcelona		ess dense, medium income, urban city, Sevilla, Lisbon, Dusseldorf, ns				
Outposts, areas of interest or private use	3-5	Vertipads	3-5	Major suburban commuting stations, private use for high net worth individuals, or in wealthy suburbs		
Near concentrations of high origin and destination points	5-10	Vertibases	3-7	Major corporate headquarters, major retail districts, and major commuting stations		
Major airports, city centres, 2-3 and major commute corridors		Vertihubs	1-2	Main airport, downtown, and major work district		
	40-60	Total landing pads	20-45			

Figure 1.4 – UAM infrastructure: scalable vertiport types [4]

Within the scope of infrastructure, it is also important to highlight command and control platforms. Unlike conventional transportation systems, UAM requires a remote platform capable of coordinating (centralized control) and supervising a high number of simultaneous flights in real time. Such a system would bring significant advantages not only to air traffic regulation, but also to urban management, facilitating coordination with other public services such as tourism, healthcare, emergency response, and security. This would enable the integration of services within an intelligent urban ecosystem [7].

# 1.4.2 Social acceptance

Although social acceptance is not considered one of the primary challenges in most publications, it has been a central focus and a significant dimension for EASA, whose role is, in fact, to act in the public interest. Figure 1.5 summarizes the main factors identified in the literature, with noise and safety ranking highest, the latter understood both as the protection of air taxi occupants and of people on the ground [4].

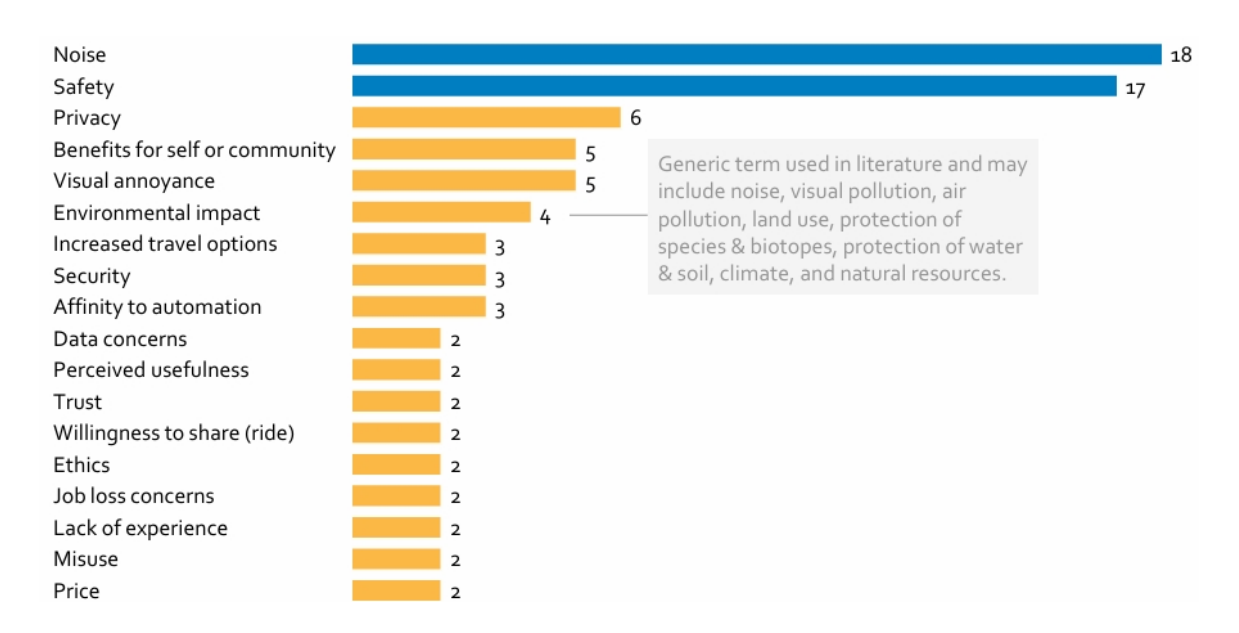


Figure 1.5 – Societal acceptance factors, in percentage [4]

For Urban Air Mobility to gain broad social and institutional acceptance, it is essential that it should not be limited in providing advantages for a wealthy elite, as is currently the case with traditional VTOLs. Instead, it is necessary to demonstrate the significant benefits that UAM can bring to the broader public. In this context, applications such as emergency response, infrastructure inspection, and traffic monitoring represent key tools for conveying the value of this technology, even to those who may not use it directly [9].

# 1.4.3 *Safety*

Safety is one of the highest priorities for any vehicle intended for Urban Air Mobility, and for this reason, it must be equipped with backup systems and redundancy. In fact, several key elements are essential to ensure the highest level of safety [7]:

- Energy redundancy, which involves the use of multiple motors and propellers (a typical example is Distributed Electric Propulsion, or DEP);
- Centralized command and control, to ensure coordinated and secure operations;
- Duplicated flight control, communication, and navigation systems, to guarantee continued functionality in case of failure;
- Complimentary autonomous operation, aimed at reducing human error associated with the presence of a pilot;
- Obstacle avoidance capability, for example through radar-based technologies;

 Intelligent self-diagnostic functionalities, for real-time assessment of the vehicle's condition.

# 1.4.4 Technology and Electric Propulsion

The concept of technology within the context of Urban Air Mobility (UAM) is complex and can be articulated across three fundamental dimensions [9]:

- 1. Communication infrastructure based on 5G networks, which enables highly precise navigation and, as a result, increased safety. However, in urban environments, its effectiveness may be limited due to the presence of tall buildings that obstruct signal transmission.
- 2. Autonomous flight technology, which, though still far from full implementation, offers numerous advantages, including cost reduction (thanks to the absence of a pilot) and increased payload capacity, thereby improving overall transport efficiency. However, as discussed in Section 1.5, removing the pilot could raise critical concerns related to employment.
- 3. Electric propulsion. Vertical take-off and landing aircraft face challenges similar to those in the automotive industry, particularly regarding battery efficiency and reliability. Minimizing the weight and volume of motors is crucial to ensuring operational efficiency, especially given that each propulsion system requires dedicated landing infrastructure and spatial configurations.

Currently, the most promising eVTOLs are equipped with lithium-ion (Li-ion) batteries, which remain the only commercially viable option despite significant limitations in terms of weight, capacity, and safety (the electrolyte fluid they contain is highly flammable). For this reason, new technologies are being developed to increase range and power while reducing both weight and charging times. In this context, solid-state batteries are emerging as one of the most promising solutions. Fuel cells represent a potential primary energy source [13], while hybrid solutions (such as internal combustion engines or gas turbines combined with electric motors) are considered less suitable for UAM due to noise and emissions. Hydrogen is also being explored as a possible propulsion source, though it currently does not appear to be destined for widespread application in this sector [2].

Figure 1.6 illustrates the projected evolution of some of these technological aspects between 2025 and 2050 [5]:

	2025	2050
Propulsion technology	Fully electric or hybrid electric based on conventional fuels	Fully electric or hybrid electric, also hydrogen-based
Level of autonomy	Onboard-Pilot / Remote-Pilot*	Highly automated autonomous
U-Space Service Level	U-space Service Level U1 (first U-space services)	U-space Service Level U2 – U3 (advanced U-space services)
Communication	Multilink communications approach relying on existing comm. infrastructure	Multilink communications approach with specific datalink
Navigation	Certified multi-sensor navigation including GNSS	Global Navigation Satellite System (GNSS) and supporting multi-sensor navigation

<sup>\*</sup> For the intra-city and mega-city use cases an onboard pilot is assumed, and for the use cases airport shuttle, suburban and intra city a remote pilot.

# Figure 1.6 – Technology scenarios [5]

It is important to emphasize that, although advancements in this field offer significant opportunities for the development of Urban Air Mobility, the rapid pace at which they are progressing, combined with the risks discussed in Section 1.5, still represents a constraint to the sustainable growth of the market.

## 1.5 UAM Risks

As with any innovation, the introduction of Urban Air Mobility also entails certain risks. Among the main concerns highlighted in the literature, or raised by industry experts, are those reported in the study "Study on the Societal Acceptance of Urban Air Mobility in Europe" [4]:

- Noise generated by vehicles during take-off, landing, and flight;
- Safety, a critical factor for public acceptance;
- Privacy, given that UAM vehicles may fly over or near residential areas;
- Visual pollution;
- Job displacement, particularly for pilots, due to automation and emerging technologies aimed at eliminating the need for a physical pilot on board;
- Environmental issues, since, even though electric aircraft produce minimal operational
  emissions, electricity must still be generated, and vehicle components must be
  manufactured, assembled, and eventually disposed of;
- Economic accessibility.

# 1.6 The concept of airspace "ownership"

Given the increasing relevance of Urban Air Mobility, urban and regional authorities have begun to assert a role in the management of low-altitude airspace, viewing it as an extension of urban space. It is important to note, however, that airspace, according to the general principles of aviation law, falls under the jurisdiction of the competent national or international authorities and does not lie within the direct remit of local entities. In this context, the scope of action for local administrations is limited to areas such as ground risk assessment and the planning of related infrastructure. To prevent potential conflicts of interest arising from the management of urban airspace, Implementing Regulation (EU) 2021/664 on the U-space<sup>1</sup> explicitly recognizes the need to ensure effective coordination with local authorities [1].

<sup>&</sup>lt;sup>1</sup> Commission Implementing Regulation (EU) 2021/664 of 22 April 2021 on a regulatory framework for the U-space, Official Journal of the European Union, L 139, 28.4.2021: 44–71 [3].

# 2. MATLAB LIVE SCRIPT

# 2.1 The updated script

The MATLAB Live Script code serves as an essential tool for evaluating the performance of the selected aircraft in this thesis work. It is therefore crucial to clarify several key aspects that define its structure, functionalities, and methods of use, in order to fully understand its potential, limitations, and role within the analysis process.

The purpose of the MATLAB Live Script is to compute the main performance characteristics of the selected aircraft, including:

- Technical polar
- Propulsive characteristics
- Climb, descent, and glide
- Endurance
- Takeoff
- Landing
- Turning.

A dropdown menu allows users to select among various aircraft models, each associated with a specific propulsion system. The algorithm is designed to operate with four distinct types of propulsion technologies: turbofan engines, turboprop engines, turbocharged engines, piston engines. Each category reflects different performance characteristics, enabling tailored aircraft selection based on the propulsion configuration.

Thanks to the work of student Giannitti [6], the code has become significantly more practical and complete in its current form. Although previous versions were already capable of accurately performing aircraft performance calculations and generating reliable outputs, the internal organization of the data exhibited notable shortcomings in terms of clarity and flexibility.

The data structure previously adopted lacked readability and a clear distinction between inputs, outputs, constant parameters, and user-configurable values. Moreover, despite being formally structured, its logical layering potential was not fully exploited: heterogeneous categories of data were often grouped within the same fields, leading to ambiguity and difficulties in consultation.

A new multi-level architecture, referred to as "AllData," was therefore developed, in which each element has been carefully named to ensure uniqueness and ease of identification. This reorganization not only enhances the accessibility and readability of information, but also enables a coherent and modular classification of data.

# 2.2 "AllData" Struct

di Turboprop & Pistons.

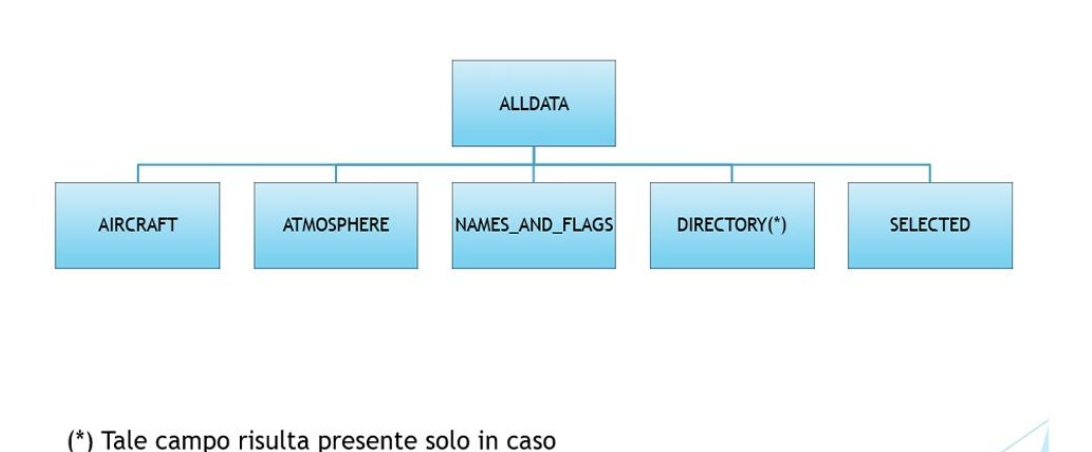


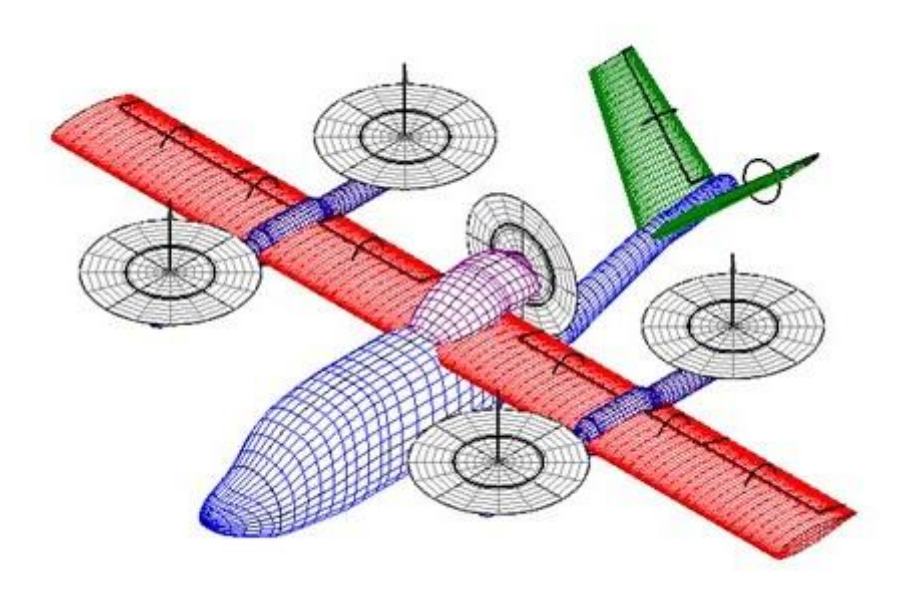
Figure 2.1 – AllData's first level [6]

As shown in Figure 2.1, the first level includes all data (both input and output) used or generated during code execution. However, for the purposes of this study, which focuses on the performance evaluation of a fixed-wing UAM vehicle, particular attention will be given to the Aircraft and Atmosphere sections. These two areas, in fact, represent the core of the performance analysis, as they contain the fundamental parameters that define the aircraft's characteristics and the environmental conditions in which it operates. By focusing on these elements, it becomes possible to examine in greater depth how variations in aircraft configuration and atmospheric properties influence the overall performance of the system.

# 2.2.1 Aircraft and Atmosphere Input Data

The following analysis concerns the input data of the aircraft selected for this study, whose performance will be examined in detail in Chapter 3.

Below is the design of the aircraft named "Seagull":



#### Select the following parameters:

Select the boarding airport altitude(m):	0
Select the arrival airport altitude(m):	0
Select a turn flight altitude(m):	1000
Select a flight altitude(m):	1500

#### Input data are here below summarized:

```
AIRCRAFT NAME: Seagull

AERODYNAMIC: CD0 = 0.036 | CLmax = 1.70 | e = 0.85 | CLmaxT0 = 2.00 | CLmax_L = 2.19 | CLg = 0.90

STRUCTURE: n_max = 3.80

GEOMETRY: S = 14.7 m2 | b = 11.5 m

POWERPLANT: Pistons | Single engine P0 = 160.0 hp | \phirev = 0.00 | SFC = 0.45 lb/(lb*hr) | Engine number = 1 | \eta = 0.70 | \etaT0 = 0.50 | \etaL = 0.50

WEIGHT: WT0 = 1640 kg | Wf = 107 kg

FLIGHT ALTITUDES: Sea Level = 0 m | Climb = 1500 m | Cruise = 1500 m | Take Off = 0 m Landing = 0 m | Selected Altitude = 1500 m | Start climb = 11 m | End climb = 1500 m
```

The data presented herein result from estimates and calculations conducted on the basis of the information currently available.

Focusing on the aerodynamic analysis of the aircraft, particular importance is given to the value of  $C_{D_0}$ , which represents the parasite drag, i.e., the drag component of the aircraft when no lift is generated. It depends on form drag (fuselage, wings, ...), skin friction, interference drag between surfaces, exposed elements (such as landing gear, antennas, ...).

This value is neither too low nor overly optimistic, as the aircraft features an aerodynamically clean geometry, with a streamlined and well-faired fuselage, and conventional tail surfaces, which minimize both form and interference drag.

Conversely, the value of  $C_{Lmax}$  refers to the clean configuration and serves as an indicator of the aircraft's capacity to generate lift effectively. From this parameter, it is possible to estimate the stall speed, defined as the minimum velocity at which the wing is capable of producing sufficient lift to sustain level flight. The formula employed for the calculation of the stall speed is as follows:

$$V_{s} = \sqrt{\frac{2W_{TO}}{\rho SC_{L_{\text{max}}}}}$$

By carrying out the calculations using a  $C_{L_{max}}$ =1.70, a stall speed of approximately  $V_s \approx 32.41$  m/s  $\approx 116.67$  km/h is obtained.

In order to compare this result with the case in which the deflected flap configuration is considered, we observe that:

- In take-off configuration ( $C_{L_{max,TO}} = 2.00$ ), the stall speed decreases to approximately 29.88 m/s, or about 107.57 km/h;
- In landing configuration ( $C_{L_{max,L}} = 2.19$ ), the stall speed is further reduced to approximately 28.55 m/s, or about 102.80 km/h.

It is clear that with flaps extended, the stall speed is reduced, thereby enhancing the aircraft's low-speed maneuverability. This characteristic proves particularly advantageous during short take-off and landing operations, as well as in confined environments, such as those typically encountered in Urban Air Mobility (UAM) applications.

It is also worth directing attention to the Oswald efficiency factor, which was computed in Excel on the basis of the following considerations:

$$C_D = C_{D_0} + KC_L^2$$

where

$$K = \frac{1}{\pi ARe}$$

By differentiating  $C_D$  with respect to  $C_L^2$  the coefficient K can be obtained, from which the Oswald efficiency factor "e" may be derived as follows:

$$e = \frac{1}{\pi AR} \frac{\partial C_L^2}{\partial C_D}$$

By plotting  $C_L^2$  (i.e., our function f(x)) as a function of  $C_D$  (our variable x) and identifying the region in which the relationship can be well approximated by a parabolic trend, where the curve locally becomes linear, the slope of this linear portion corresponds to the Oswald efficiency factor.

Figure 2.2 illustrates the methodology just described, along with the corresponding dataset and the resulting value of the parameter "e".

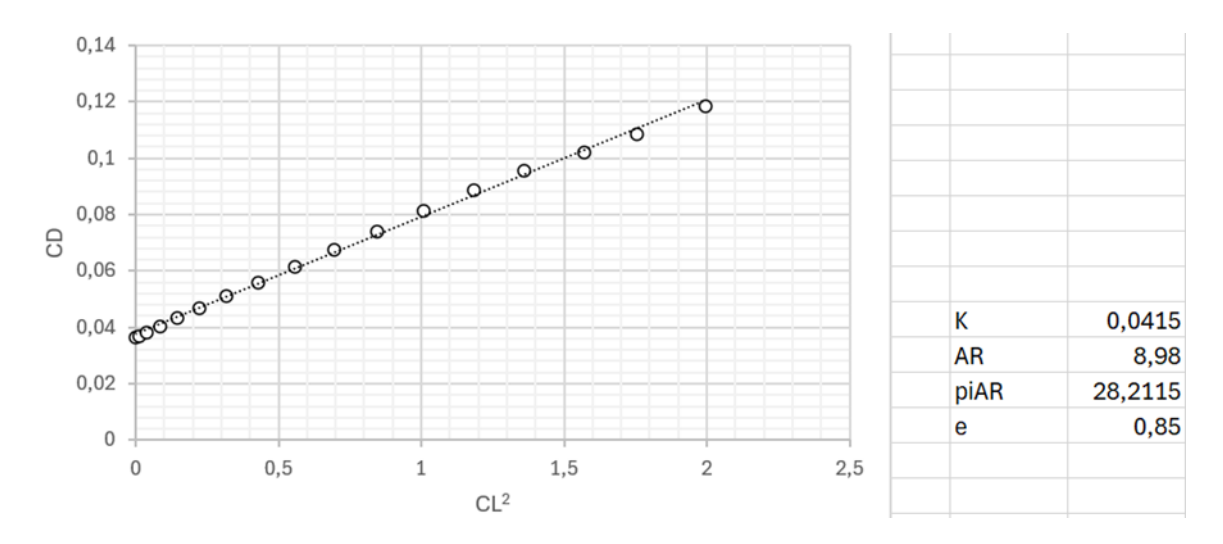


Figure 2.2 – Plot of  $C_D$  VS  $C_L^2$  for the calculation of the Oswald efficiency factor

From a structural standpoint, based on the measurements obtained from Figure 2.3, it was possible to determine the wing surface area S and the wingspan b, from which the Aspect Ratio (AR) was calculated using the following relation:

$$AR = \frac{b^2}{S} = \frac{11,5^2}{14,7} \approx 8,98$$

This value represents a favorable trade-off between aerodynamic efficiency and structural feasibility. For an aircraft intended for low-speed flight with short take-off and landing capabilities, such a value is considered optimal. The moderate wingspan and wing area contribute to maintaining a structurally compact configuration, suitable for operations in urban environments, while still ensuring sufficient lift generation at low speeds.

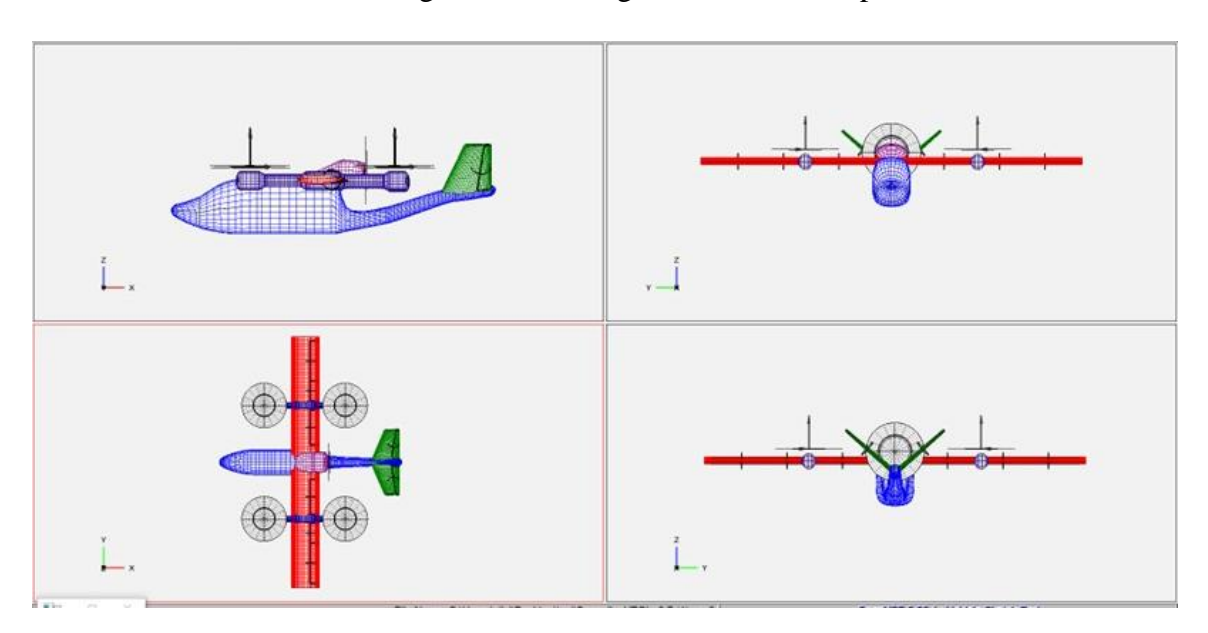


Figure 2.3 – Complete aircraft with propellers

With regard to engine selection, the Rotax 916 iS proves to be particularly well-suited for a fixed-wing UAM aircraft with horizontal takeoff. This 160 hp engine is compact and lightweight, key characteristics for an urban air mobility platform, as they allow for increased payload capacity or extended range. The specific fuel consumption (SFC) of 0.45 lb/(lb·hr) is relatively low, contributing to a reduction in the required onboard fuel weight. Additionally, thanks to its turbocharger and intercooler, the engine is capable of maintaining full power up to 15,000 feet. Overall, the Rotax 916 iS offers an optimal balance between performance, weight, reliability, and operating costs, making it an efficient and coherent choice for a fixed-wing UAM vehicle [12].

# 3. AIRCRAFT PERFORMANCE EVALUATION

The following section presents the performance results of the "Seagull", which is the subject of this study. The collected data offer a detailed overview of the vehicle's operational capabilities, enabling an assessment of its effectiveness in relation to the predefined objectives. The analyses conducted provide a valuable contribution to understanding the system's performance under real-world operating conditions.

The first available performance results generally refer to the aircraft's maximum performance, such as rate of climb, maximum level flight speed, maximum range, etc. These values represent the theoretical upper limits achievable under optimal conditions.

Then follow the performances calculated and measured under specific conditions, determined by usually imposed constraints on parameters such as altitude, speed, throttle setting, or aircraft configuration. These results, which reflect real operational scenarios, provide a comprehensive overview of the aircraft's performance.

# 3.1 Technical polar

In the analysis of the characteristic points we start with the evaluation of point E. The other points are correlated thanks to the following table:

Punto	CD/CD <sub>0</sub>	CL/CL <sub>E</sub>	E/E <sub>MAX</sub>	V/V <sub>E</sub>	T/T <sub>E</sub>	II/II <sub>P</sub>
P	4	$\sqrt{3} = 1.732$	$\frac{\sqrt{3}}{2} = 0.866$	$\frac{1}{\sqrt[4]{3}} = \frac{1}{1.316}$	$\frac{2}{\sqrt{3}} = 1.155$	1
E	2	1	1	1	1	$\frac{\sqrt[4]{27}}{2} = 1.140$
A	4/3	$\frac{1}{\sqrt{3}} = 0.577$	$\frac{\sqrt{3}}{2} = 0.866$	$\sqrt[4]{3} = 1.316$	$\frac{2}{\sqrt{3}} = 1.155$	$\sqrt{3} = 1.732$

Here are summarized the data points for different flight altitudes:

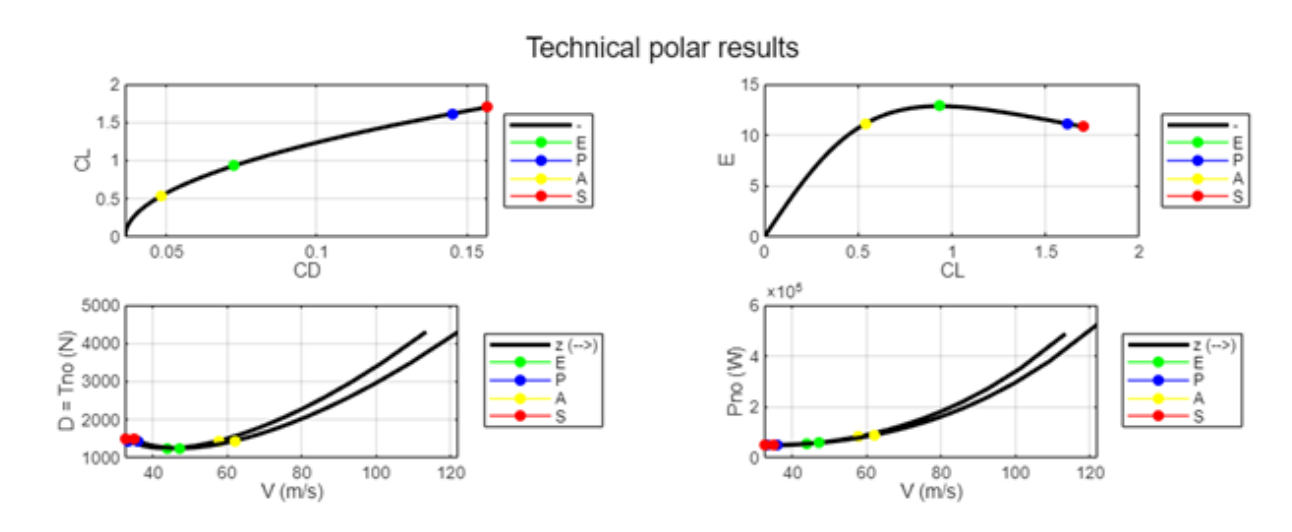
SEA LEVEL =0 m
SEA\_LEVEL\_RESULTS = 4×8 table

	Punto	CL	CD	E	V (m/s)	D (kN)
1	'E'	'0.93'	'0.07'	'12.85'	'43.75'	'1.25'
2	'P'	'1.62'	'0.15'	'11.13'	'33.25'	'1.45'
3	'A'	'0.54'	'0.05'	'11.13'	'57.58'	'1.45'
4	'S'	'1.70'	'0.16'	'10.84'	'32.41'	'1.48'

CRUISE ALTITUDE =1500 m CRUISE RESULTS = 4×8 table

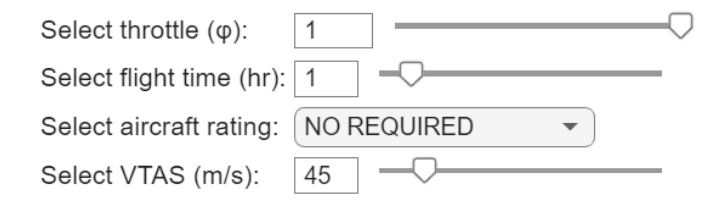
	<del>-</del>						
	Punto	CL	CD	E	V (m/s)	D (kN)	
1	'E'	'0.93'	'0.07'	'12.85'	'47.08'	'1.25'	
2	'P'	'1.62'	'0.15'	'11.13'	'35.77'	'1.45'	
3	'A'	'0.54'	'0.05'	'11.13'	'61.96'	'1.45'	
4	'S'	'1.70'	'0.16'	'10.84'	'34.87'	'1.48'	

The graphs were calculated at sea level and cruise (1500m) flight altitudes.



# 3.2 Propulsive characteristics

Select these values for the calculation of propulsive characteristics:



WARNING! Aircraft max velocity is shown in chapter 5

Below are shown aircraft propulsive characteristics at selected altitude and selected flight conditions:

```
T = 1603.05 N = 360.26 lbf = 163.41 kgf P = 72137.22 W = 72.14 kW = 96.74 hp Fuel = 35.26 lt = 28.21 kg = 62.19 lb For the calculation of the performance, it was used the following rating: PA = PA0*\sigma*\phi*EnginesNumber
```

# 3.3 Climb, Descent and Glide

#### 3.3.1 Best CLIMB

Performance at sea level flight altitude is below summarized:

```
Sea level = 0 m, \phi = 1.00, Vp = 33.25 m/s
Point P --> Optimal RateOfClimb = 2.20 m/s = 433.68 ft/min; \gamma = 0.07 rad = 3.80 deg
```

Performance at selected flight altitude is below summarized:

```
Selected flight altitude= 1500 m, \phi = 1.00, Vp = 35.77 m/s
Point P --> Optimal RateOfClimb = 1.27 m/s = 249.73 ft/min; \gamma = 0.04 rad = 2.03 deg
```

#### 3.3.2 Actual Climb

Performance at selected flight altitude is below summarized:

```
Selected flight altitude= 1500 m, \phi = 1.00, VTAS = 45.00 m/s RateOfClimb = 0.97 m/s = 190.32 ft/min; \gamma = 0.02 rad = 1.23 deg The rate of climb was calculated considering the Thrust and the Drag at the selected altitude and selected flight conditions, using the formula RC=V*(T-D)/W
```

#### 3.3.3 Controlled Climb

Below is shown the throttle value for selected RC and VTAS values. Take care that not all combination are feasible

Select RC value (m/s):	0.5	$\bigcirc$
Select VTAS (m/s):	40	$\overline{}$

WARNING! In order to have a power surplus and thus achieve rate of climb, it is necessary to select a VTAS within the range of v\_min and v\_max(max velocity is shown in chapter 5) v min = 34.87 m/s

As the minimum speed, we have taken the stall speed of selected flight altitude.

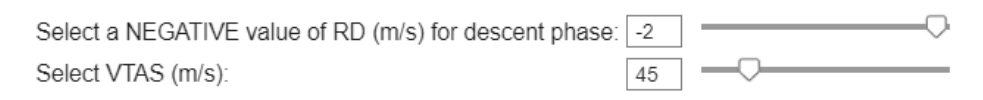
Selected flight altitude: 1500 m

Throttle ( $\phi$ ) value = 0.843

Angle of climb gamma = 0.71627 deg.

#### 3.3.4 Controlled Descent

Below is shown the throttle value for selected Rate of Descent RD and VTAS values at given altitude. Take care that not all combination are feasible.



Selected flight altitude: 1500 m Aircraft descent performance Throttle (φ) value = 0.338 Angle of descent gamma = -2.5475 deg.

# 3.3.5 Ceiling AEO

1)	Below	are	shown	the	extrapolated	ceilings

```
Select throttle (φ) for high flight altitude climb:

Select throttle (φ) for low flight altitude climb:

O.9

Absolute ceiling = 1200 m
Service ceiling = 1200 m
(Extrapolated flight altitude: 1200 m (RC = 0.9893m/s) and 1200 m (RC = 1.4512 m/s).

2) Below is shown the exact ceiling:

SigmaTT = 0.69197
Absolute ceiling = 3674 m
SigmaTT has been calculated using Sigma_TT = (Dp*Vp_sl/(P0*eta_p*K_V))^(2/3)
```

# 3.3.6 Climb flight time

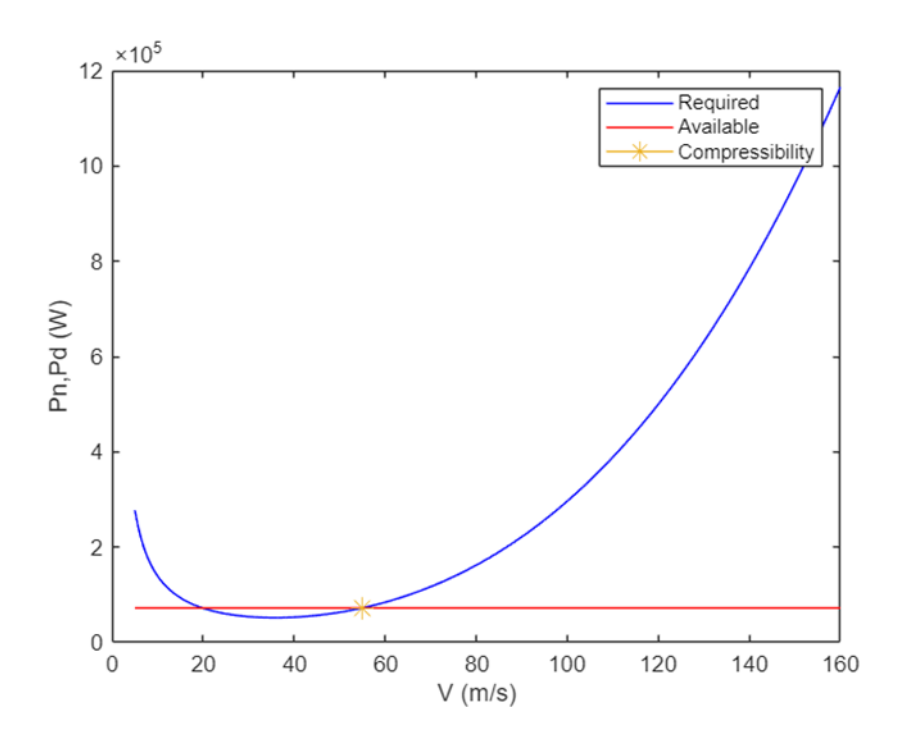
Climb flight time to reach cruise flight altitude is shown below:

Select throttle (φ) for starting climb flight altitude: 1	<b>─</b> ▽
Select throttle (φ) for ending climb flight altitude: 1	<del>-</del>
Climb flight time is calculated between 11 m and 1500 m, RC is ca conditions. $t=882\ s=14.7\ min$	lculated in point P

# 3.4 Level Flight

Max aircraft velocity, calculated in cruise conditions, is shown below:

Cruise flight altitude: 1500 m
Select throttle (φ) for cruise flight altitude:
Select 'ON' if you want to see level flight graphs: ON
Cruise flight altitude: 1500 m Max sustainable level flight speed is (analytic approach): 55.45 m/s = 199.63 km/h Max sustainable level flight speed is (graphic approach): 54.90 m/s = 197.64 km/h ANALYTIC M = 0.17 GRAPHIC M = 0.16



# 3.5 Autonomies

Aircraft autonomies are shown below.

```
Selected flight conditions: the aircraft is flying at an altitude of 1500 m at 45 m/s.
v_{in} = 45.00 \text{ m/s}
h_{in} = 1500 \text{ m}
For this type of aircraft, the Breguet formulas that allow us to calculate endurance and
En = 53.5*eta*CL^1.5*sqrt(2*rho*S)/(SFC*CD)*(1/sqrt(W1)-1/sqrt(W0)) - R = 1.5*eta*CL^1.5*sqrt(2*rho*S)/(SFC*CD)*(1/sqrt(W1)-1/sqrt(W0)) - R = 1.5*eta*CL^1.5*eta*CL^1.5*eta*CL^1.5*eta*CL^1.5*eta*CL^1.5*eta*CL^1.5*eta*CL^1.5*eta*CL^1.5*eta*CL^1.5*eta*CL^1.5*eta*CL^1.5*eta*CL^1.5*eta*CL^1.5*eta*CL^1.5*eta*CL^1.5*eta*CL^1.5*eta*CL^1.5*eta*CL^1.5*eta*CL^1.5*eta*CL^1.5*eta*CL^1.5*eta*CL^1.5*eta*CL^1.5*eta*CL^1.5*eta*CL^1.5*eta*CL^1.5*eta*CL^1.5*eta*CL^1.5*eta*CL^1.5*eta*CL^1.5*eta*CL^1.5*eta*CL^1.5*eta*CL^1.5*eta*CL^1.5*eta*CL^1.5*eta*CL^1.5*eta*CL^1.5*eta*CL^1.5*eta*CL^1.5*eta*CL^1.5*eta*CL^1.5*eta*CL^1.5*eta*CL^1.5*eta*CL^1.5*eta*CL^1.5*eta*CL^1.5*eta*CL^1.5*eta*CL^1.5*eta*CL^1.5*eta*CL^1.5*eta*CL^1.5*eta*CL^1.5*eta*CL^1.5*eta*CL^1.5*eta*CL^1.5*eta*CL^1.5*eta*CL^1.5*eta*CL^1.5*eta*CL^1.5*eta*CL^1.5*eta*CL^1.5*eta*CL^1.5*eta*CL^1.5*eta*CL^1.5*eta*CL^1.5*eta*CL^1.5*eta*CL^1.5*eta*CL^1.5*eta*CL^1.5*eta*CL^1.5*eta*CL^1.5*eta*CL^1.5*eta*CL^1.5*eta*CL^1.5*eta*CL^1.5*eta*CL^1.5*eta*CL^1.5*eta*CL^1.5*eta*CL^1.5*eta*CL^1.5*eta*CL^1.5*eta*CL^1.5*eta*CL^1.5*eta*CL^1.5*eta*CL^1.5*eta*CL^1.5*eta*CL^1.5*eta*CL^1.5*eta*CL^1.5*eta*CL^1.5*eta*CL^1.5*eta*CL^1.5*eta*CL^1.5*eta*CL^1.5*eta*CL^1.5*eta*CL^1.5*eta*CL^1.5*eta*CL^1.5*eta*CL^1.5*eta*CL^1.5*eta*CL^1.5*eta*CL^1.5*eta*CL^1.5*eta*CL^1.5*eta*CL^1.5*eta*CL^1.5*eta*CL^1.5*eta*CL^1.5*eta*CL^1.5*eta*CL^1.5*eta*CL^1.5*eta*CL^1.5*eta*CL^1.5*eta*CL^1.5*eta*CL^1.5*eta*CL^1.5*eta*CL^1.5*eta*CL^1.5*eta*CL^1.5*eta*CL^1.5*eta*CL^1.5*eta*CL^1.5*eta*CL^1.5*eta*CL^1.5*eta*CL^1.5*eta*CL^1.5*eta*CL^1.5*eta*CL^1.5*eta*CL^1.5*eta*CL^1.5*eta*CL^1.5*eta*CL^1.5*eta*CL^1.5*eta*CL^1.5*eta*CL^1.5*eta*CL^1.5*eta*CL^1.5*eta*CL^1.5*eta*CL^1.5*eta*CL^1.5*eta*CL^1.5*eta*CL^1.5*eta*CL^1.5*eta*CL^1.5*eta*CL^1.5*eta*CL^1.5*eta*CL^1.5*eta*CL^1.
eta*E/SFC*log(W0/W1)*603.5
To maximize En, it is necessary to set point P as the attitude, while to maximize R, point
E must be set as the attitude.
Aircraft maximum autonomies at fixed h_in altitude are:
En max = 5.56 hr
R max = 813.7 km
Aircraft actual autonomies at fixed h in altitude:
En = 5.09 hr
R = 810.4 \text{ km}
the actual autonomies has been calculated by fixing the actual attitude
The final speed will be:
v_{fin} = 43.51 \text{ m/s} = 156.63 \text{ km/h}
Aircraft maximum autonomies at fixed v_in:
En max = 5.48 hr
R max = 813.7 km
Aircraft actual autonomies at fixed v_in are:
En = 5.00 hr
R = 810.4 \text{ km}
the actual autonomies has been calculated by fixing the actual attitude
The final altitude will be:
h_fin = 115 m
```

## 3.6 Take-off

At first, choose the temperature of the airport the airplane is leaving:

```
Boarding airport temperature (°C) 15

At the altitude of 0 m and at a temperature of 15 °C, the total distances that the airplane needs to take off correctly are:

Sg = 526 m

Sair = 132 m

Stot= Sg + Sair = 658 m

At the same altitude and in standard conditions (T= 288.15 K) the total distances that the airplane needs to take off correctly are:

Sg = 527 m

Sair = 132 m

Stot_stan= Sg_stan+Sair_stan = 659 m
```

# 3.7 Landing

Landing performance are shown below:

Arrival airport temperature (°C) 15

At the altitude of 0 m and at a temperature of 15 °C, the total distances that the airplane needs to land correctly are:
Sa = 136 m
Sflare = 53 m
Sfr = 62 m
Sg = 196 m
Stot=Sa+Sflare+Sfr+Sg = 446 m
At the same altitude and in standard conditions (T= 288.15 K) the total distances that the airplane needs to land correctly are:
Sa\_stan = 136 m
Sflare\_stan = 53 m
Sfr\_stan = 62 m
Sg\_stan = 196 m
Stot\_stan=Sa\_stan+Sflare\_stan+Sfr\_stan+Sg\_stan = 446 m

# 3.8 Turn

Select load factor	1.1
Select VTAS (m/s):	45
Select aircraft rating:	No rating required ▼

keep in mind that for this aircraft n\_max = 3.80

#### 3.8.1 Best Turn

Turn best sustainable performance at sea level flight altitude is below summarized:

```
Sea level = 0 m
Minimum turn speed sustainable = 38.95 m/s
Minimum turn radius sustainable = 148.40 m
Max rate of turn sustainable = 15.04 deg/s
Max bank angle sustainable = 46.18 deg
Max load factor sustainable = 1.44
```

Turn best sustainable performance at selected turn flight altitude is below summarized:

```
Selected turn flight altitude= 1000 m
Minimum turn speed sustainable = 38.95 m/s

Minimum turn radius sustainable = 182.54 m
Max rate of turn sustainable = 12.23 deg/s
Max bank angle sustainable = 40.27 deg
Max load factor sustainable = 1.31
```

#### 3.8.2 Actual Turn

Turn performance at selected turn flight altitude is below summarized:

```
Selected turn flight altitude= 1000 m
Turn speed = 45.00 m/s
load factor = 1.10
Turn radius = 450.45 m
Rate of turn = 5.72 deg/s
Bank angle = 24.62 deg
```

# 3.9 Influence of Parasite Drag on Performance

The performance presented above, for the purposes of this study, refers to a fixed value of the parasite drag coefficient, equal to  $C_{D_0}$ = 0.0363. However, it is interesting to analyze what happens when this value varies. This section reports a brief parametric analysis of the maximum performance as  $C_{D_0}$  increases, considering values between 250 and 450 drag counts. The results shown in Figure 3.1 are the outcome of an iterative update of the aircraft's "AllData" structure with the current values of the parasite drag coefficient, executed using the Matlab live script code.

	h (km)	0	1,5					
CD0	L/D max	RoC max (fpm)	RoC max (fpm)	V max (m/s	En max (hr)	Range max (km)	Glide range max (km	V max (km/h)
0,025	15,48	486	306	64,04	6,11	980,5	23,22	230,5
0,030	14,13	461	279	59,71	5,83	895,1	21,195	215,0
0,035	13,08	439	255	56,25	5,61	828,7	19,62	202,5
0,040	12,24	419	234	53,38	5,43	775,2	18,36	192,2
0,045	11,54	401	215	50,95	5,27	730,9	17,31	183,4

Figure 3.1- Maximum performance values as a function of  $C_{D_0}$ 

The results of this study are now examined through their graphical representation.

# 3.9.1 Influence on Maximum Efficiency

As can be observed in Figure 3.2, the maximum efficiency of the aircraft decreases with increasing  $C_{D_0}$  that is, with increasing parasite drag.

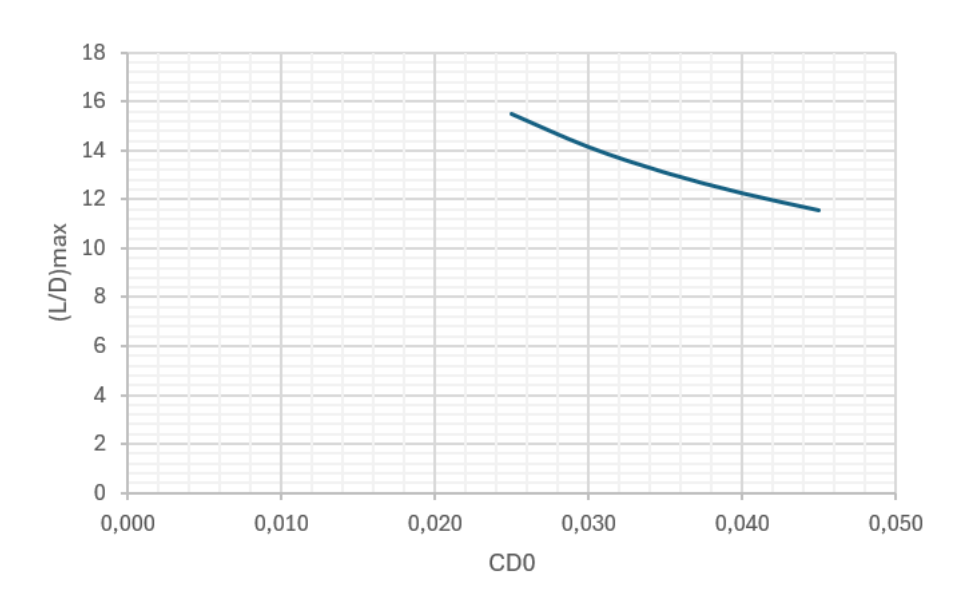


Figure 3.2 – Maximum Efficiency vs.  $C_{D_0}$ 

Indeed, a higher  $C_{D_0}$  leads to an increase in the total drag (D) which in turn reduces the maximum lift-to-drag ratio  $(L/D)_{max}$ .

# 3.9.2 Influence on Maximum Speed

The maximum speed is limited by the available power. As the parasite drag increases, and therefore the total drag, more power is required to overcome it. However, since the available power is fixed/limited, the maximum speed, as shown in Figure 3.3, exhibits a decreasing trend.

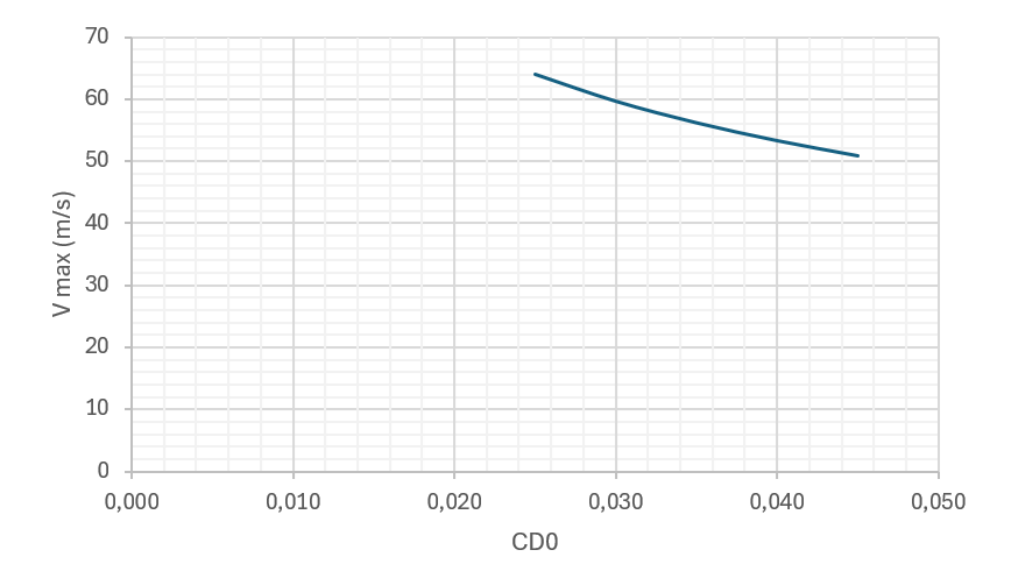


Figure 3.3 – Maximum Speed vs.  $C_{D_0}$ 

# 3.9.3 Influence on Maximum Rate of Climb

The maximum rate of climb is determined by the margin between the available power and the power required. As the parasite drag coefficient increases, and with available power fixed/limited, the required power rises, thereby reducing the available margin and, consequently, the rate of climb, as illustrated in Figure 3.4.

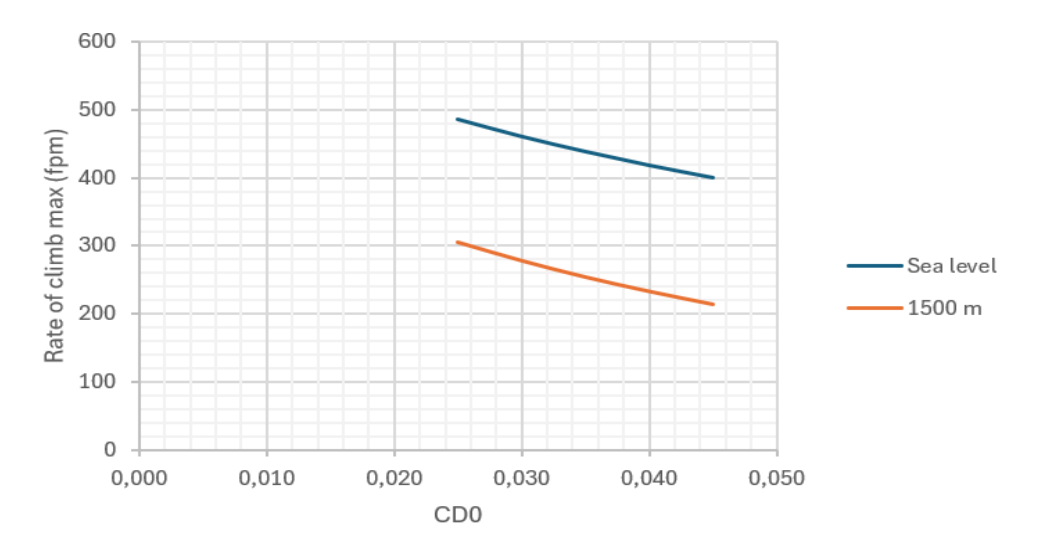


Figure 3.4 – Rate of climb max vs.  $C_{D_0}$ 

At an altitude of 1500 meters, the available power is already lower than at sea level, making this decrease even more pronounced.

# 3.9.4 Influence on Maximum Endurance

Maximum endurance is achieved by combining speed and configuration in such a way as to minimize power consumption. A high value of  $C_{D_0}$  results in increased drag, forcing the engine to operate at higher power settings to maintain the same speed. This leads to greater fuel consumption. Consequently, as  $C_{D_0}$  increases, maximum endurance tends to decrease, as shown in Figure 3.5.

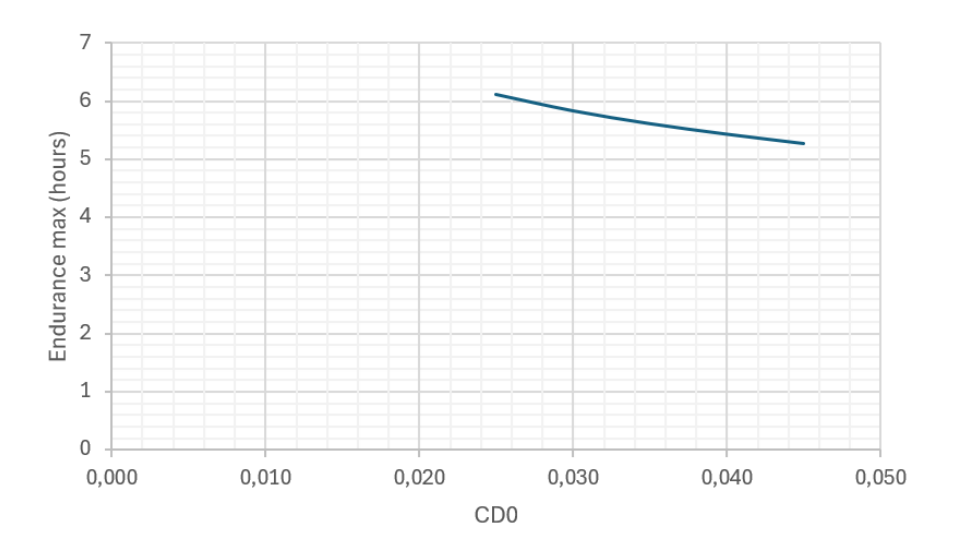


Figure 3.5 – Endurance max vs.  $C_{D_0}$ 

To maximize endurance, an aircraft must operate at the velocity corresponding to the minimum power required. This minimum power is highly sensitive to parasite drag due to the following reasons:

- Parasite drag increases with the square of the airspeed;
- As the zero-lift drag coefficient ( $C_{D_0}$ ) increases, the entire power-required curve shifts significantly upward.

Consequently, the minimum power required increases more rapidly than the power required at higher speeds. Since endurance is inversely proportional to the minimum power required, any increase in  $C_{D_0}$  leads to a marked reduction in endurance.

In summary, even small increases in  $C_{D_0}$  can substantially raise the minimum power required and significantly degrade endurance.

# 3.9.5 Influence on Maximum Range

Maximum range depends on the lift-to-drag ratio (L/D): the higher this ratio, the greater the distance the aircraft can travel for a given amount of fuel. As shown in Subsection 3.9.1, an increase in  $C_{D_0}$  leads to higher aerodynamic drag, resulting in a reduction of the (L/D) ratio. Consequently, the maximum range also decreases, as illustrated in Figure 3.6.

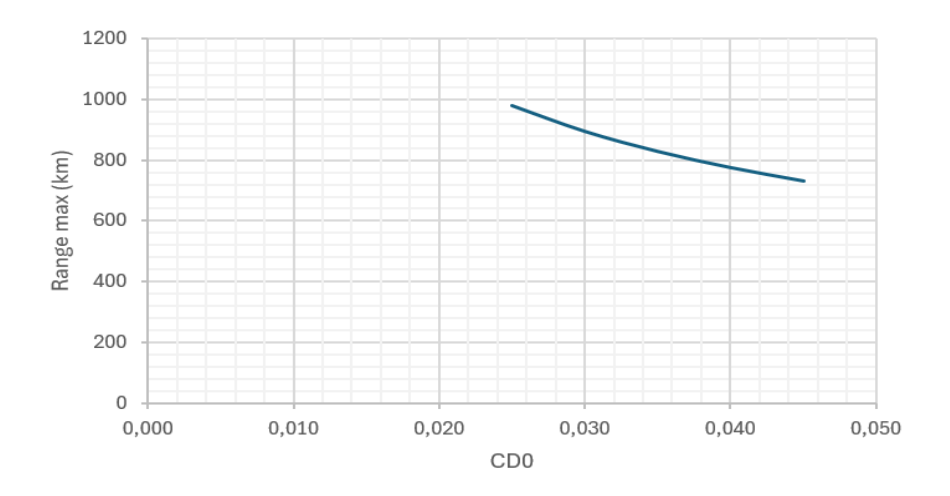


Figure 3.6 – Maximum Range vs.  $C_{D_0}$ 

# 3.9.6 Influence on Maximum Range in Glide

The maximum glide range depends entirely on the lift-to-drag ratio (L/D) during gliding flight. As shown in Figure 3.7, an increase in the parasite drag coefficient leads to higher aerodynamic drag, which reduces the (L/D) ratio. As a result, the distance that can be covered in a glide decreases accordingly.

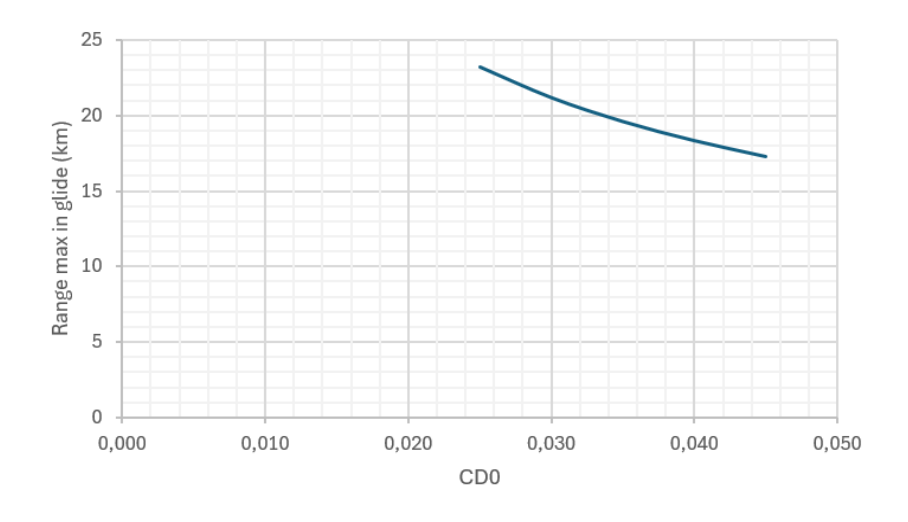


Figure 3.7 – Maximum Range in Glide vs.  $C_{D_0}$ 

# 4. Conclusion

This study provided a comprehensive overview of what, in the coming years, could become the so-called "flying taxis." After analyzing their main characteristics, both technical and structural aspects were highlighted, as well as theoretical and regulatory considerations. The various applications, along with objectives aimed at mitigating the issues associated with their introduction, supported by technological development, demonstrate that their integration into everyday urban life is not as distant as commonly perceived.

An analysis of the performance of the "Seagull" experimental aircraft in cruise configuration (hovering propellers not considered) was therefore conducted using a MATLAB Live Script code. This analysis revealed aerodynamic and propulsive behavior consistent with that expected for a light aircraft equipped with a piston engine. The results obtained showed good reliability in the main operational regimes: level flight, climb, descent, range, take-off, landing, and turning. In particular, the study showed that the aircraft's level flight performance, including its maximum sustainable speed, aligns with the installed power and design characteristics. The take-off and landing distances were found suitable for short runway operations. The climb and descent performance properly account for the power loss with increasing altitude, while the turn performance remains within the imposed structural and aerodynamic limits.

The final parametric study, conducted by varying the parasite drag coefficient ( $C_{D_0}$ ), exhibited behavior consistent with theoretical expectations. It is noteworthy to emphasize the effects of increasing parasite drag, as this can indeed happen during real-world missions due to the presence of rivets, surface irregularities, manufacturing imperfections, or surface contamination. These factors, often neglected in ideal theoretical analyses, contribute to an increase in  $C_{D_0}$ , with detrimental effects on the overall performance of the aircraft, as demonstrated by the decreasing trends in the performance curves presented.

In conclusion, performance calculation overall represents a useful tool for the preliminary analysis of the aircraft's flight behavior. Further refinements could include, for example, a dynamic estimate of fuel consumption or the introduction of variable atmospheric models, in order to make this study even more reliable and complete.

# **Bibliography**

- [1] Agouridas V., Biermann F., Czaya A., Richter D., Stemmler J., Stęchły J., Witkowska-Konieczny A., Kumar R., Patatouka E. (2021) Urban Air Mobility and Sustainable Urban Mobility Planning, European Platform on Sustainable Urban Mobility Plans (ELTIS).
- [2] Antignani, R. (2024). Urban Air Mobility: che cos'è e perché rivoluzionerà il modo in cui ci spostiamo in città. EconomyUp. Accessibile su: <a href="https://www.economyup.it/mobilita/urban-air-mobility-che-cose-e-perche-rivoluzionera-il-modo-in-cui-ci-spostiamo-in-citta/">https://www.economyup.it/mobilita/urban-air-mobility-che-cose-e-perche-rivoluzionera-il-modo-in-cui-ci-spostiamo-in-citta/</a>.
- [3] European Commission (2021) Commission Implementing Regulation (EU) 2021/664 of 22 April 2021 on a regulatory framework for the U-space, Official Journal of the European Union, L 139, 28.4.2021: 44–71.parasite
- [4] European Union Aviation Safety Agency (EASA), McKinsey & Company (2021), Study on the societal acceptance of Urban Air Mobility in Europe.
- [5] German Aerospace Center (DLR), (2024) The Future of Urban Air Mobility. The Integration of Air Taxis into Urban Airspace: Findings from HorizonUAM, a Research Project of the German Aerospace Center (DLR).
- [6] Giannitti M. (2023) MATLAB live script for aircraft performance, Elaborato di Laurea, Università degli Studi di Napoli Federico II, a.a. 2022–2023. Relatore: Prof. Ing. Pierluigi Della Vecchia.
- [7] Hang E. (2020) The Future of Transportation: White Paper on Urban Air Mobility System.
- [8] Raymer D. P. (2006) Aircraft Design: A Conceptual Approach. AIAA Education Series, 4th ed.
- [9] Roland Berger (2018) Urban Air Mobility, The rise of a new mode of transportation, Focus.
- [10] Roskam J. (1973) Methods for Estimating Drag Polars of Subsonic Airplanes. University of Kansas, Department of Aerospace Engineering.
- [11] https://www.easa.europa.eu/en/what-is-uam
- [12] <a href="https://www.flyrotax.com/it/products/916-is-c">https://www.flyrotax.com/it/products/916-is-c</a>
- [13] <a href="https://uam.fev.com/">https://uam.fev.com/</a>